Liquid Crystals
Publication details, including instructions for authors and subscription information:
http://www.informaworld.com/smpp/title~content=t713926090

Molecular dynamics of a liquid-crystalline polymer with laterally fixed mesogenic side groups

Franz Josef Bormuth[a]; Wolfgang Haase[a]
[a] Institut für Physikalische Chemie der Technischen Hochschule Darmstadt, Darmstadt, F.R. Germany

To cite this Article Bormuth, Franz Josef and Haase, Wolfgang(1988) 'Molecular dynamics of a liquid-crystalline polymer with laterally fixed mesogenic side groups', Liquid Crystals, 3: 6, 881 — 891
To link to this Article: DOI: 10.1080/02678298808086545
URL: http://dx.doi.org/10.1080/02678298808086545

LIQUID CRYSTALS, 1988, VOL. 3, NOS. 6 AND 7, 881–891

Molecular dynamics of a liquid-crystalline polymer with laterally fixed mesogenic side groups

by FRANZ JOSEF BORMUTH and WOLFGANG HAASE
Institut für Physikalische Chemie der Technischen Hochschule Darmstadt, Petersenstraße 20, D-6100 Darmstadt, F.R. Germany

The long range molecular dynamical behaviour of liquid-crystalline side chain polymers with the mesogenic groups linked laterally to the backbone have been studied by using dielectric relaxation spectroscopy over a broad temperature and frequency range. The samples were oriented homeotropically and homogenously by electric and magnetic fields and the relaxations were recorded during alignment and with the fully aligned samples. By fitting the data to theoretical relaxation curves, accurate relaxation parameters could be determined, allowing us to perform a comparison with end-fixed liquid-crystalline side chain polymers on the one hand and with low molecular weight liquid crystals on the other. The relaxation in homeotropic alignment for the laterally fixed compound has more analogies in some aspects, for example, the relaxation time distribution, with low molecular weight liquid crystals than with the corresponding end-fixed compounds, though the activation energy is very large (241 kJ/mol). We relate this to the length of the rigid mesogenic unit and the resulting stronger repulsion by the neighbouring side chains during reorientation. In homogeneous alignment the relaxation is very broad and also has a large activation energy. Different molecular processes are related to this relaxation regime. The relationship between the different relaxation processes and the molecular structure is discussed.

1. Introduction

Dielectric spectroscopic investigations of end-fixed liquid-crystalline side chain polymers in recent years [1–10] have revealed two main relaxation regimes in the liquid-crystalline phase. The first lies at lower frequencies and is restricted to homeotropically or incompletely homogeneously aligned samples. It is called the δ relaxation and is assigned to 180° rotations of the mesogenic side group around an axis perpendicular to its long axis. The other, at higher frequencies, is observed mainly in homogeneous orientation (**E** perpendicular to the axis of alignment). For incomplete or homeotropic orientation it is often covered by the δ relaxation. It can be interpreted as a combined process including main chain and side chain motions, but this is still under discussion. Recently some attempts have been made to perform a quantitative analysis and decomposition of the dielectric spectra into single processes [9, 10]. However, there are still many open questions concerning the fundamental features of molecular dynamics of liquid-crystalline polymer systems.

In order to obtain more insight into this problem we have in the past varied the strength and position of polar groups in the compounds as well as the structure of the main chain [7, 9]. Another solution is to vary the principal structure of the systems. This is the scope of the present study. The compound investigated here has the same polymer backbone as compounds investigated previously [9], but with lateral attachment of the mesogenic side groups to the spacer, leading to optical biaxiality [13]. If the motional models for end-fixed crystalline polymers can be applied to this

side-fixed system, we expect characteristic changes in the relaxation parameters, which might help in interpreting the microscopic phenomena.

2. Theory

The frequency dependence of the complex dielectric permittivity in the two main orientations can be described for uniaxial, polymeric systems

$$\varepsilon_{\parallel}(\omega) = \varepsilon_{\parallel}^{\infty} + G/3kT(\mu_l^2(1 + 2S)F_{\parallel}^{1}(\omega) + \mu_t^2(1 - S)F_{\parallel}^{t}(\omega)) + \Delta\varepsilon_{\parallel}(S, \mu_g)F_g(\omega), \quad (1\,a)$$
$$(A_{00}) \qquad (A_{01}) \qquad (B)$$

$$\varepsilon_{\perp}(\omega) = \varepsilon_{\perp}^{\infty} + G/3kT(\mu_l^2(1 - S)F_{\parallel}^{1}(\omega) + \mu_t^2(1 + S/2)F_{\parallel}^{t}(\omega)) + \Delta\varepsilon_{\perp}(S, \mu_g)F_g(\omega), \quad (1\,b)$$
$$(A_{10}) \qquad (A_{11}) \qquad (C)$$

where $\varepsilon_{\parallel}^{\infty}$, $\varepsilon_{\perp}^{\infty}$ are the limiting high frequency permittivities, μ_t, μ_l mean the transverse and longitudinal dipole components of the mesogenic group, $\Delta\varepsilon(S, \mu_g)$ means the strength of the main chain relaxation, μ_g is an average dipole moment of the monomeric unit in the main chain, S is the order parameter, and $F_{\parallel,\perp,g}(\omega)$ are relaxation functions of the different dipole components. G is a factor containing the dipole density.

The molecular interpretation of the first two terms in equations (1 *a*) and (1 *b*) has been described by [10] and [12]. The third term has been added tentatively by us to account for main chain motions. Its relaxation strength is mostly dependent on the average dipole moment of the main chain units and only weakly dependent on the alignment state.

From equation (1) we expect three relaxation regimes in each orientation with different locations on the frequency scale. A_{00} is assumed to be identical with the δ process in homeotropic orientation. The relaxation times of A_{01}, A_{10} and A_{11} should obey the relation $\tau_{01} \gtrsim \tau_{10} \gtrsim \tau_{11}$ according to Nordio *et al.* [12]. They have never been observed separately for polymeric liquid crystals.

3. Experimental

The structure and phase transitions of the compound

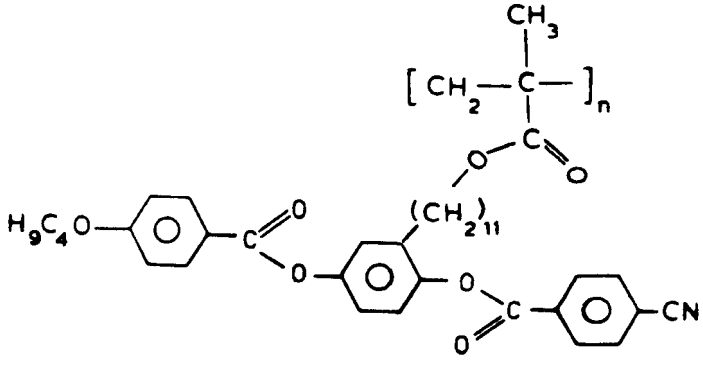

are: glass 36°C nematic 75°C isotropic.

The polymer was prepared and characterized by Hessel and Finkelmann [11] and used by us without further treatment. The different experimental techniques, which have been described previously [6, 9], allow us to cover a frequency range of 0·1 Hz to 10 MHz. Over the whole range we used the same shielded plate condensor, where

the sample is introduced by capillary force. The spacing is 75 μm and the sample area is about 80 mm^2. The sample temperature could be varied from -50°C to $+200$°C with an accuracy of 0·1°C. Homeotropic alignment was achieved by a magnetic field of 1·2 T and an additional electric field applied to the electrodes. It had a strength of approximately 10 kV/cm and a frequency of 100 Hz. This gave good alignment, which was checked by polarization microscopy. For homogeneous alignment the additional electric field had a frequency of 200 kHz, where the dielectric anisotropy is negative. However, this gave only partial alignment, as we shall discuss later. It is probably due to the small negative dielectric anisotropy of the compound.

It is helpful to know approximately the components of the dipole moment parallel and perpendicular to the long axis of the mesogen. We have made an estimate based on the vector addition model outlined by Klingbiel *et al.* [15] using experimentally determined group dipole moments. This method leads to the values, μ_l(longitudinal) = 4·59 D; μ_t(transverse) = 2·6 D. For comparison we shall quote some data for a low molecular weight liquid crystal which is analogous to the mesogenic group of the polymer except for a terminal hexoxy group instead of the butoxy group; these data are taken from the literature [14].

4. Results

X-ray diffraction patterns were taken from samples aligned by an electric field and with drawn fibres. Both methods gave identical pictures, typical for nematic phases. For the drawn fibres, the side groups align parallel to the direction of draw. Since the main chains can be assumed to align in the draw direction, this means that main chains and mesogenic units prefer a parallel arrangement.

The temperature dependence of the real part of the permittivity at a frequency of about 0·01 kHz (see figure 1) shows for homeotropic alignment a very small relaxation step above the glass temperature and a very large relaxation step setting in at approximately 50°C and reaching its unrelaxed value of $\varepsilon' \sim 9{\cdot}5$ at about 70°C. For homogeneous alignment only one broad relaxation is observed, which sets in at the glass temperature reaching a maximum value of $\varepsilon' \sim 5{\cdot}5$. The isotropic permittivity is 7·6 with a falling tendency.

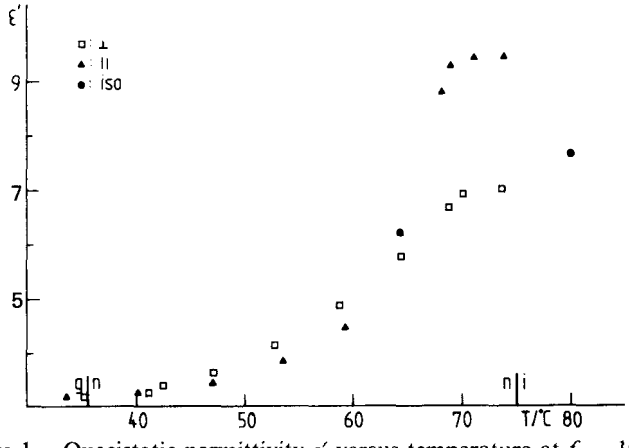

Figure 1. Quasistatic permittivity ε' versus temperature at $f = 10$ Hz.

Table 1. Comparison with the low molecular weight analogue [14]. ε'_{max} at $f = 10$ Hz; f_r is the relaxation frequency for homeotropic alignment; T_m is the crystallization or glass point temperature; $\varepsilon - \varepsilon_\infty$, β, E_a are the relaxation strength, distribution parameter and activation energy for homeotropic alignment, respectively.

	ε'_{max} (∥)	ε'_{max} (⊥)	$\log(f_r/\text{Hz})$ $T = (T_m + 20)/°C$	$\log(f_r/\text{Hz})$ $T = (T_m + 40)/°C$	$\varepsilon - \varepsilon_\infty$	β	$E_a/\text{kJ/mol}^{-1}$
Polymer	9·5	5·5	0·08	2·3	5·2	0·93	241
Low molecular weight	9·8	4·4	6·0	6·5	≈6	≈1	46–87†

† Dependent on the phase.

Comparing the unrelaxed ε' values with the low molecular weight analogue (see table 1), we see that the homeotropic values are nearly the same, while the homogenous value is larger for the polymer; however,

$$\bar{\varepsilon} = 1/3(\varepsilon_{\parallel} + 2\varepsilon_{\perp})$$

does not show a step at the clearing point.

The experimental relaxation curves, of which some representative examples are shown in figures 2 and 4, were fitted using a superposition of only two Fuoss–Kirkwood functions, for they show no marked separation. The mathematical form is

$$\varepsilon'' = 2\varepsilon_m/(\cosh(\beta \ln(f/f_r))), \tag{2}$$

where ε_m is the maximum of ε'', β is the distribution parameter and f_r is the relaxation frequency. Since, according to equation (1), there are at least three or, if incomplete alignment is taken into account, even five different relaxation processes in each main

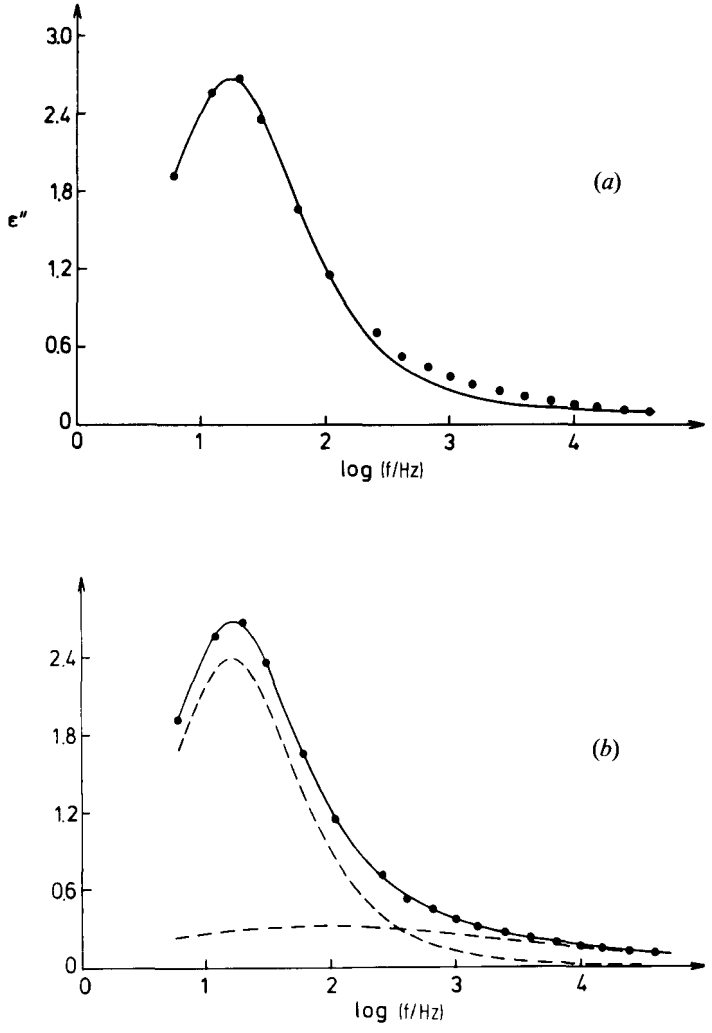

Figure 2. Absorption curves for homeotropic alignment at $T = 68{\cdot}3°C$. Solid and dotted lines are the fitted curves according to equation (2); (*a*) one line fit; (*b*) two lines fit.

orientation, this implies the assumption that these processes except A_{00} either coincide or are located at frequencies beyond our measurement range. This is supported by the fact that only two relaxation regimes have hitherto been found for liquid-crystalline polymers.

4.1. *Homeotropic alignment*

The determined parameters for two line fits as well as for one line fits are presented in table 2. There is some difference regarding the values of the dominant relaxation for the two procedures, but a better approximation of the experimental points is achieved by two line fits. The dominant relaxation must be identified with term A_{00} in equation (1 *a*), while the high frequency contribution contains, in addition to the term B and perhaps A_{01}, also the term A_{11} if the homeotropic alignment is not quite perfect. Since the last absorption is very broad and unresolved, we restrict our discussion at this stage to A_{00}. It has the following properties:

(i) the distribution parameter is very close to 1, which means that the relaxation time distribution is very small, even smaller than for end-fixed side chain polymers [5, 9]; moreover, it does not broaden with decreasing temperature;

(ii) the relaxation strength is similar to the analogous low molecular weight liquid crystal (table 1).

Table 2. Fit parameters for homeotropic orientation. In the first four rows the parameters for the two line fit are shown; ε_m is the maximum of the absorption curve, f_r, ε_m and $\varepsilon - \varepsilon_\infty$ have the same meaning as in table 1. The next four rows show the parameters for the one line fit. In the last row we give the square root of the sum of squares divided by the number of measurement points, Δ, to indicate the quality of the fits.

T/°C	$f_{r,1}$/Hz	$\varepsilon_{m,1}$	β_1	$(\varepsilon - \varepsilon_\infty)_1$	$f_{r,2}$/Hz	$\varepsilon_{m,2}$	β_2	$(\varepsilon - \varepsilon_\infty)_2$	Δ
74·1	67	2·03	0·97	4·2	126	0·47	0·38	2·5	0·0050
71·2	33	2·3	0·98	4·7	88	0·35	0·29	2·4	0·011
68·3	16	2·39	0·90	5·3	86	0·32	0·30	2·1	0·0026
65·6	8·3	2·32	0·93	5·0	26	0·31	0·23	2·7	0·0055
74·1	78	2·31	0·86	5·4	—	—	—	—	0·019
71·2	34	2·51	0·89	5·6	—	—	—	—	0·021
68·3	17	2·57	0·84	6·1	—	—	—	—	0·015
65·6	8·6	2·51	0·86	5·8	—	—	—	—	0·021

4.2. *Homogeneous alignment*

Figure 3 shows the absorption curves for different homogeneous alignment conditions. Two line fits reveal a successive reduction of the homeotropic contribution and an increase in the broad absorption curve at higher frequencies. Since the homeotropic contribution does not disappear we assume that homogeneous alignment is still incomplete, which is also indicated by the behaviour of the static permittivity ε' in figure 1. The best evaluation method under these circumstances is to perform two line fits, where the parameters of one curve are fixed to the homeotropic values except for the maximum ε_m. The parameters obtained by this method are given in table 3. Two representative experimental curves are shown in figure 4.

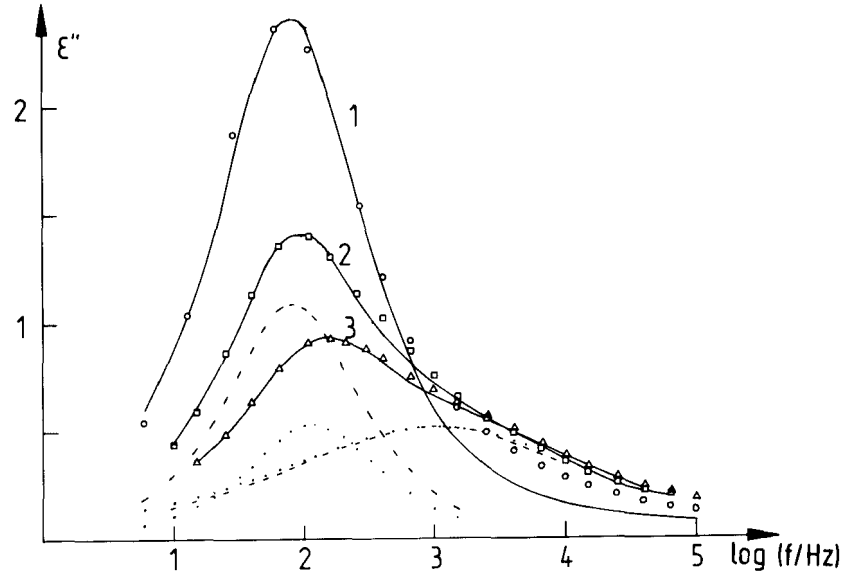

Figure 3. Development of absorption curves with alignment conditions. Curve 1, homeotropic alignment; curve 2, partly homogeneous alignment with electric field $E = 10\,\text{kV/cm}$; curve 3, partly homogeneous alignment with $E = 10\,\text{kV/cm}$ and additional $B = 1{\cdot}2\,\text{T}$, annealed for 24 hours below the clearing point. Fitted curves are represented by dashed lines for 2 and dotted lines for 3.

Table 3. Fit parameters for homogeneous alignment. $f_{r,1}$ and β_1 were fixed during the fit procedure. Parameters as in table 2.

T/°C	$f_{r,1}$/Hz	$\varepsilon_{m,1}$	β_1	$(\varepsilon - \varepsilon_\infty)_1$	$f_{r,2}$/Hz	$\varepsilon_{m,2}$	β_2	$(\varepsilon - \varepsilon_\infty)_2$	Δ
73·7	64	0·25	0·95	0·5	550	0·72	0·45	3·2	0·0090
70·2	36	0·66	0·95	1·4	330	0·53	0·39	2·7	0·0039
64·4	7.6	0·55	0·93	1·2	81	0·52	0·33	3·2	0·0021
58·8	1·4	0·48	0·90	1·1	16	0·55	0·32	3·4	0·0038

According to Attard and Williams [10] we can obtain an estimate for the homogeneous orientation order parameter S_d by assuming that homeotropic alignment is complete. Then S_d is given by

$$S_d = (3\Delta\varepsilon_{1,\text{PA}} - \Delta\varepsilon_{1,\text{A}})/2\Delta\varepsilon_{1,\text{A}}, \tag{3}$$

where $\Delta\varepsilon_1 = 2\varepsilon_{m1}/\beta_1$ is the relaxation strength for term A_{00} in equation (1 *a*) and the subscripts PA and A mean parallel homogeneous and complete homeotropic alignment, respectively. We find $S_d \approx -0{\cdot}30$ for the best alignment curves ($S_d = -0{\cdot}5$ means complete homogeneous alignment).

4.3. *Activation diagram*

In the activation diagram (see figure 5 (*a*)) the following features should be noted:

(i) the homeotropic relaxation frequencies obey an Arrhenius law over the whole range; the activation energy is relatively large (241 kJ/mol) and decreases strongly in the isotropic phase (150 kJ/mol);

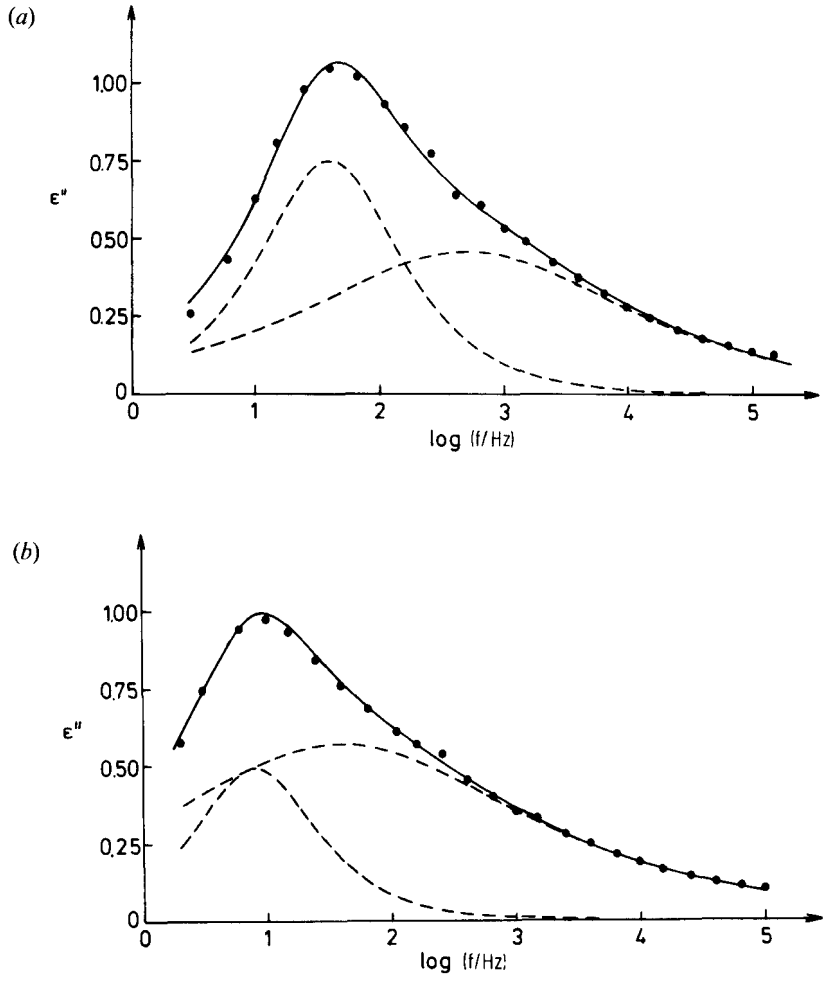

Figure 4. Absorption curves for homogeneous alignment at (*a*) 70·2°C and (*b*) 64·4°C. Solid and dotted lines are the fitted curves.

(ii) the homogeneous relaxation frequencies also have a linear temperature dependence, however the errors of each point is relatively large; the apparent activation energy of each point is very large (350 kJ/mol).

4.4. *Glass state*

Below the glass transition we found another weak relaxation process characterized by a distribution parameter β of about 0·2 and a relaxation strength of approximately 0·32. Its relaxation frequencies show Arrhenius behaviour with an activation energy of ~ 56 kJ/mol (see figure 5 (*b*)).

5. Discussion

Here we shall refer to our previous work with end-fixed liquid-crystalline side chain polymers, especially to the compounds with acrylate backbones [5, 7] and methacrylate backbones [9] and with cyanophenylbenzoate side chains. The interpretations

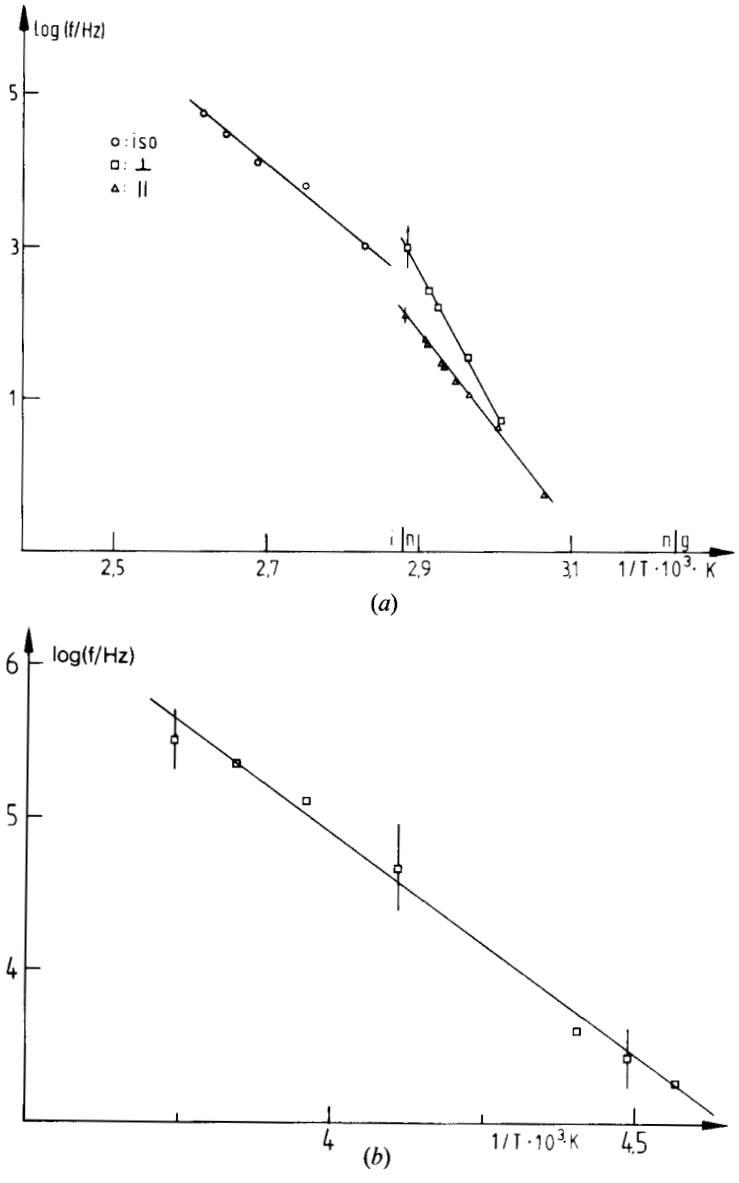

Figure 5. Activation diagram for (*a*) nematic and isotropic, (*b*) glass phase.

given for these end-fixed compounds must be modified for the present side-fixed compounds because

(i) the spacer is much longer (11 CH_2 groups compared to 6 CH_2 groups leading to largely independent motions of the mesogenic groups);

(ii) the lateral attachment of the mesogens should hinder rotations around their long axes;

(iii) X-ray diffraction indicates that the side groups align preferentially parallel to the main chain.

5.1. *Homeotropic alignment*

The dominant process is assigned to the term A_{00} in equation (1 *a*), which means that it is an end-to-end reorientation of the mesogenic group. This is in agreement with the large relaxation strength which is similar to the low molecular weight analogue (cf. table 1). However, the molecular motion is not analogous with the δ process described for end-fixed compounds [9] concerning the axis of rotation of the mesogenic group. We assume that the side groups are essentially reorienting about the point of attachment to the spacer. The resulting motion resembles very much the low frequency relaxation for low molecular weight liquid crystals [9]. This model is in agreement with the weak coupling between main chain and mesogen as well as with the small relaxation time distribution as compared with the end-fixed liquid-crystalline polymer with methacrylate backbone [9] and the Arrhenius-like behaviour of relaxation frequencies. The activation energy of this process is relatively high, which is at first sight difficult to understand. Looking at figure 6, where we have sketched the main chain and the side chains in the correct proportions, we see that the side chains overlap considerably with their neighbours. A reorientation then requires overcoming of many intermolecular potential barriers among each other and with the neighbouring spacer groups. This could explain the large activation energy.

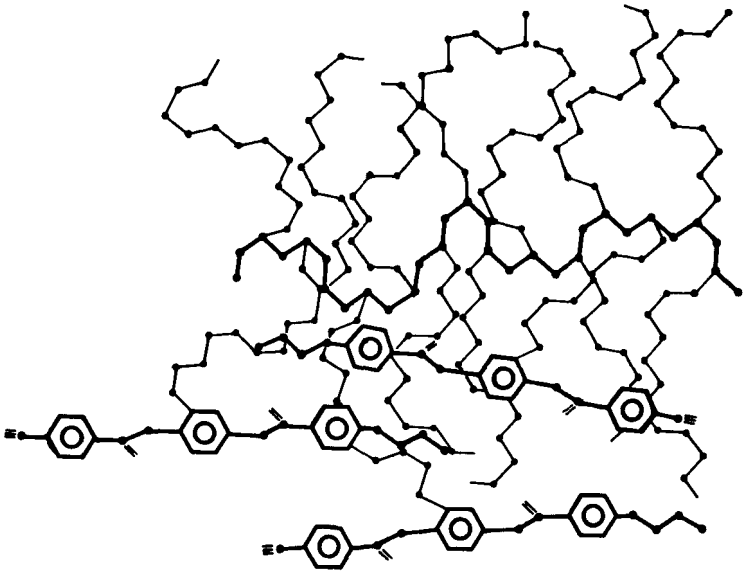

Figure 6. Schematic picture of the proposed molecular arrangement in the nematic state. Only few mesogenic side groups are shown.

In the isotropic phase the activation energy decreases to values comparable with the end-fixed compounds.

5.2. *Homogeneous orientation*

According to equation (1 b), three processes with comparable relaxation strengths should contribute to the homogeneous dielectric spectrum. The term A_{10} can be described as a precession of the mesogenic molecule around the director, term A_{11} as a rotation around its long axis and term C as the micro-brownian motion of the main

chain. Since our experimental curves are rather unspecific, we cannot decompose them into these single relaxations.

For a discussion of the relative contributions of these processes to the relaxation spectrum, the lateral attachment is an important aspect. Especially the rotation around the long axis A_{11} is hindered by this attachment, which should result in a larger activation energy and smaller relaxation frequency and relaxation strength compared with the end-fixed compounds. Indeed, if we compare these values with those for the end-fixed methacrylate of [9], we find a reduction of the relaxation frequency by a factor of about 10 and an activation energy of 180 kJ/mol for the end-fixed compound compared with 350 kJ/mol for the side-fixed. Also the relaxation strength for the end-fixed compound is larger.

The experimental data do not allow a more detailed characterization at present. This would require investigations of related compounds, for example with a shorter spacer.

5.3. *Glass state*

The features of the relaxation in the glass state are very similar to the local process in the glass state which was observed for end-fixed side chain polymers [5–7]. We ascribe it to 180° rotations of the phenyl rings around the 1–4 axis, which become active dielectrically through the neighbouring ester bridges. Such motions have also been observed by deuteron N.M.R. spectroscopy [16].

We thank Professor Finkelmann, Dr. Hessel and P. Herr from Freiburg University for supplying us with the liquid-crystalline polymer. Financial support by DFG is gratefully acknowledged.

References

[1] ZENTEL, R., STROBL, G. R., and RINGSDORF, H., 1985, *Macromolecules*, **18**, 960.
[2] KRESSE, H., KOSTROMIN, S., and SHIBAEV, V. P., 1982, *Makromol. Chem. rap. Commun.*, **3**, 509.
[3] PRANOTO, H., HAASE, W., FINKELMANN, H., and KIECHLE, U., 1984, *15. Freiburger Arbeitstagung Flüssigkristalle, Conference Proceedings*, paper 12.
[4] HAASE, W., and PRANOTO, H., 1985, *Polymeric Liquid Crystals*, edited by A. Blumstein (Plenum Press).
[5] HAASE, W., PRANOTO, H., and BORMUTH, F. J., 1985, *Ber. Bunsenges. phys. Chem.*, **89**, 1229.
[6] PRANOTO, H., BORMUTH, F. J., HAASE, W., KIECHLE, U., and FINKELMANN, H., 1986, *Makromol. Chem.*, **187**, 2453.
[7] BORMUTH, F. J., HAASE, W., and ZENTEL, R., 1987, *Molec. Crystals liq. Crystals*, **148**, 1.
[8] ATTARD, G. S., WILLIAMS, G., GRAY, G. W., LACEY, D., and GEMELL, P. A., 1986, *Polymer*, **27**, 185.
[9] BORMUTH, F. J., and HAASE, W., 1987, *Molec. Crystals liq. Crystals*, **153**, 207.
[10] ATTARD, G. S., and WILLIAMS, G., 1986, *Liq. Crystals*, **1**, 253.
[11] HESSEL, F., and FINKELMANN, H., 1985, *Polym. Bull.*, **14**, 375.
[12] NORDIO, P. L., RIGATTI, G., and SEGRE, U., 1973, *Molec. Phys.*, **25**, 129.
[13] HESSEL, F., and FINKELMANN, H., 1986, *Polym. Bull.*, **16**, 158.
[14] NJEUMO, N. R., PARNEIX, J. P., LEGRAND, C., TINH, N. H., and DESTRADE, C., 1986, *J. Phys., Paris*, **47**, 903.
[15] KLINGBIEL, R. T., GENOVA, D. J., CRISWELL, T. R., and VAN METER, J. P., 1974, *J. Am. chem. Soc.*, **56**, 7651.
[16] PSCHORN, U., SPIESS, H. W., HISGEN, B., and RINGSDORF, H., 1986, *Makromol. Chem.*, **187**, 2711.